INTENSE EMISSION OF SMITH-PURCELL RADIATION AT THE FUNDAMENTAL FREQUENCY FROM A GRATING EQUIPPED WITH SIDEWALLS

J.T. Donohue, Centre d'Etudes Nucléaires de Bordeaux-Gradignan, Université Bordeaux 1, CNRS/IN2P3, BP 120, 33175 Gradignan, France
J. Gardelle, P. Modin, CEA, CESTA, F-33114 Le Barp, France

Abstract

The two-dimensional theory of the Smith-Purcell free-electron laser predicts that coherent Smith-Purcell radiation can occur only at harmonics of the frequency of the evanescent wave that is resonant with the beam. Particle-in-cell simulations have shown that in a three-dimensional context, where the lamellar grating has sidewalls, coherent Smith-Purcell radiation can be copiously emitted at the fundamental frequency, for a well-defined range of beam energy. An experiment at microwave frequencies has confirmed this prediction. The power output is considerably greater than for the previously observed emission at the second harmonic, in agreement with three-dimensional simulations. The dependence of frequency on beam energy and emission angle is also in good agreement with three-dimensional theory and simulations. Provided that a reduction in scale can be achieved, a path is open to coherent Smith-Purcell radiation at Terahertz frequencies.

INTRODUCTION

Radiation emitted by an electron passing over a diffraction grating was observed long ago by Smith and Purcell [1], and the idea of using this effect in a free-electron laser (FEL) has been proposed by numerous authors [2, 3, 4, 5, 6]. Renewed interest in the Smith-Purcell (SP) FEL followed the analysis of the dispersion relation for lamellar gratings by Andrews and Brau (AB) [7]. This relation links the axial wave number k to the frequency ω of the evanescent surface that propagates along the grating. They pointed out that the interaction between an initially continuous electron beam and this evanescent wave could lead to bunching at the frequency of the wave, giving rise to what they called coherent SP radiation. Such bunching would increase the intensity of the SP radiation, and by its periodicity, constrain the frequency of the radiation to be a multiple of the frequency of the evanescent wave. However, that frequency was necessarily inferior to the minimum allowed frequency, as determined by the well-known SP relation,

$$\lambda = \frac{c}{f} = \frac{L}{|n|}\left(\frac{1}{\beta} - \cos\theta\right), \qquad (1)$$

where λ denotes the wavelength of the radiation of frequency f produced at angle θ with respect to the beam direction, L is the period, c is the speed of light, β is the electron's relative axial velocity, and the integer n is the order of diffraction. However, if the bunching were strong enough, it might contain harmonics whose frequencies are SP allowed. Under these circumstances, monochromatic radiation at these frequencies would be observed at the angles corresponding to Eq. (1). The evanescent wave was expected to escape from the ends of the grating, according to AB. Using an approach based on finding singularities of the reflection matrix, Kumar and Kim [8] obtained results similar to those of AB. Simulations using the particle-in-cell code "MAGIC" [9] performed by two of us [10] and by Dazhi Li and collaborators [11] supported the AB scenario. A common aspect of all these works was that the analysis was two-dimensional (2-D), i.e., the electromagnetic fields did not depend on the coordinate parallel to the grating's grooves.

Although theory and simulations predicted emission of radiation at the second and perhaps higher harmonics of the evanescent wave, experimental confirmation was obtained only recently [12]. This was a demonstration experiment in the microwave domain, and used a wide (10 cm) flat and intense (180A) electron beam to produce bunching at 4.6 GHz, and radiation at 9.2 GHz. The ratio of radiated power to beam power was approximately 0.15%. A follow-up experiment used a very narrow slit to reduce the current and found that a start current of approximately 20 A/m was needed to achieve gain [13].

GRATINGS WITH SIDEWALLS

An experiment had previously used gratings equipped with conducting sidewalls at the ends of the grooves [14]. Two of the present authors presented a generalization of the AB 2-D dispersion relation to 3-D for a grating with sidewalls [15]. In this study, the sidewalls rise infinitely high above the grating. In practice, of course, they rise only a small distance above the top of the grating. However, if the evanescent height of the wave is less than the sidewall height, the approximation of an infinite wall is valid. A number of measurements with a signal analyzer of the grating used in our experiments confirmed the predictions of the theory, as did 3-D simulations performed with "MAGIC". Li and collaborators had also performed simulations for sidewall with gratings [16].

ISBN 978-3-95450-126-7

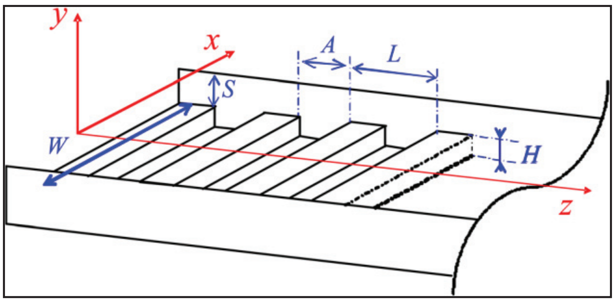

Figure 1: Sketch of grating with sidewalls, showing parameters and choice of axes.

A sketch of the grating is shown in Figure 1, with our choice of the axes. The grating is described by five parameters, the period L, groove width A, groove depth H, separation between sidewalls W and height of the sidewall above the grating top, S. We summarize the results of the theory briefly. The components H_x, E_z and E_y of the 2-D AB model all get multiplied by a factor $\cos(qx)$. Since these fields must vanish at the perfectly conducting sidewalls, $qW/2$ must be an odd multiple of $\pi/2$. Thus q must be an odd multiple of π/W. There are also anti-symmetric modes, where the cosine is replaced by sine. For these $qW/2$ must be an integer multiple of π. Working out the details, we found that the generalization of the AB dispersion relation from 2-D to 3-D is made by writing

$$\omega_{3-D}(k,q)=\sqrt{(\omega_{2-D}(k))^2+(cq)^2} \quad .$$

Here $\omega_{2\text{-D}}(k)$ denotes the frequency associated with k in the AB theory. Results similar to this may be found in the work of Kim and Kumar [17] and in much older work by McVey and co-workers on gratings inserted in waveguides [18].

DISPERSION RELATIONS

We show in Figure 2 an explicit representation of both the 2-D and 3-D dispersion relations for the grating we used in our simulations. In fact, the dispersion relation is periodic in k, with period denoted by $K = 2\pi/L$. We display here only the first Brillouin zone, but the reader should imagine an infinite chain of them extending in both directions. Instead of ω we show the frequency f (GHz) as a function of k. The grating parameters were $L = 2$ cm, $A = H = 1$ cm and $W = 4$ cm. The green curve is for 2-D, while the blue curve is the lowest 3-D mode ($q = \pi/W$). The light lines (in black) indicate the phase velocity of light traveling in forward and backward directions. These correspond to

$$f = ck/2\pi \quad \text{and} \quad f = c(K-k)/2\pi ,$$

respectively. These light lines may be generalized to all Brillouin zones by writing

$$f = c(k-mK)/2\pi \quad \text{and} \quad f = c(mK-k)/2\pi ,$$

where m denotes any positive integer.

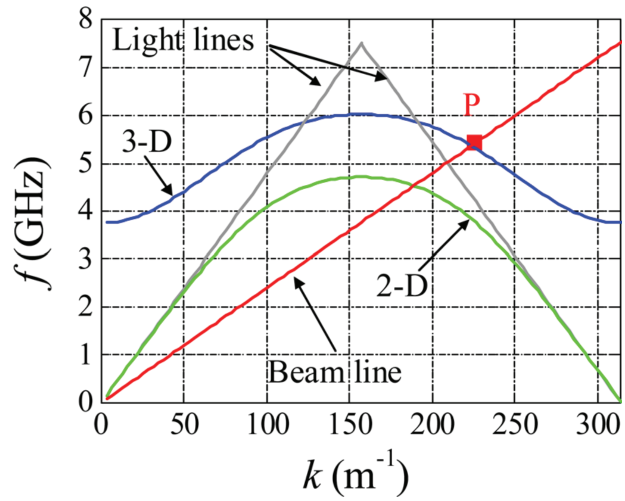

Figure 2: Dispersion relations for 2-D and 3-D.

The red line indicates the beam line, $2\pi f = \beta ck$. An electron on this line will see a constant phase as it propagates with relative axial velocity β., and thus will be in resonance with the surface wave. The intersection of the beam line with the dispersion relation determines the operating point, indicated in the figure by P.

If we solve for the intersection of the beam line with an arbitrary backward light line, we find

$$f/c = \lambda^{-1} = m/L(1/\beta+1) ,$$

which is just Eq. (1) with $|n| \to m,\ \theta \to \pi$. Similarly, the intersection with an arbitrary forward light line yields

$$f/c = \lambda^{-1} = m/L(1/\beta-1) ,$$

which is just Eq. (1) with $|n| \to m,\ \theta \to 0$. Thus the evanescent wave can correspond to an allowed SP frequency only if the intersection P occurs outside the triangle formed by the light lines in any Brillouin zone. One sees that the 2-D curve lies inside the triangle, so the intersection occurs there. In contrast, some portion of the 3-D curve must lie outside the triangle, for any finite value of W. By choosing a beam energy such that the intersection falls outside, we can get the bunching to occur at an allowed SP frequency. Since bunching on the fundamental frequency is usually much greater than bunching on a harmonic, we expect copious emission of SP radiation. Note that the intersection P occurs not far from the backward light line, which means that the radiation will be emitted near the backward direction.

ISBN 978-3-95450-126-7

THREE-DIMENSION SIMULATIONS

To see how a grating with sidewalls would function, we performed "MAGIC" 3-D simulations for the grating described above [19]. In Figure 3 we display a "MAGIC" simulation contour map at fixed time of the magnetic field component B_x in the y-z plane at $x = 0$. The color scale has been chosen to maximize visual contrast. In reality the field in the grooves is much higher than the fields well above the grating. The 30 period grating is visible at the bottom of the figure.

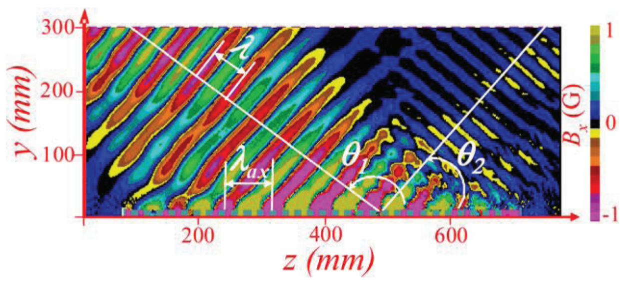

Figure 3: "MAGIC" simulation contour map of B_x in the median y-z plane

The continuous electron beam, (5 A, 1 mm thick, 3.5 cm wide, 0.5 mm above the grating) is emitted from a thin cathode and absorbed at the downstream end by a beam-stop. The simulation operates at the point P, with $f = 5.2$ GHz and wave number $k = 230\ \mathrm{m}^{-1}$. The dominant component in the evanescent Floquet wave has a negative wave number k-K, which corresponds to a backward-moving wave whose axial wavelength $\lambda_{ax} = 7.6$ cm. This wave is clearly visible in the neighborhood of the grating, where λ_{ax} is indicated. The free wavelength, $\lambda = 5.7$ cm, is also indicated. What is remarkable is the intense coherent SP radiation emitted at angle θ_1 of about 140°. This radiation moves in synchrony with the superluminous backward surface wave. One thus has $\cos\theta_1 = \lambda/\lambda_{ax}$. Also visible is the second harmonic, emitted at angle θ_2.

In Figure 4 we show an instantaneous phase-space density plot of electrons in the z-T (kinetic energy) plane.

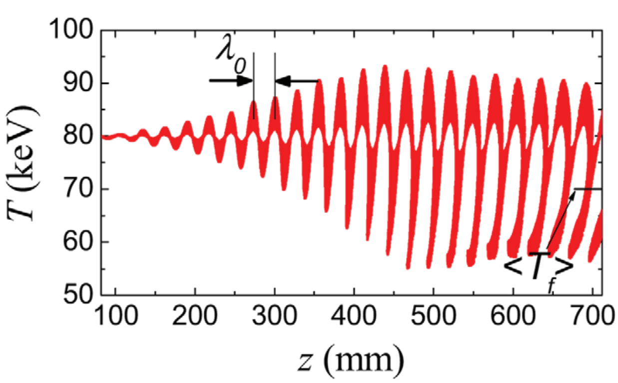

Figure 4: Phase-space density in the z-T plane.

At the far end of the grating the mean final energy $\langle T_f \rangle$is 70 keV. Given the current of 5 A, this suggests a power loss of 50 kW. The "MAGIC" estimate of power flowing through the back, top and sides of the simulation volume totaled 44 kW, which is roughly consistent with the energy lost by the beam. The efficiency is thus in the range 10-12 %. However, "MAGIC" estimates the power radiated on the second harmonic as only 350 W, for efficiency < 0.1. We note also the wavelength of the oscillations, denoted λ_0 in the figure, is about 28 mm, which is consistent with the expected value, $k = 230\ \mathrm{m}^{-1}$.

EXPERIMENTAL RESULTS

In order to test the simulation we performed an experiment with a grating having the same parameters as in the previous simulation, except that it had only 20 periods [20]. Single shot operation was used.

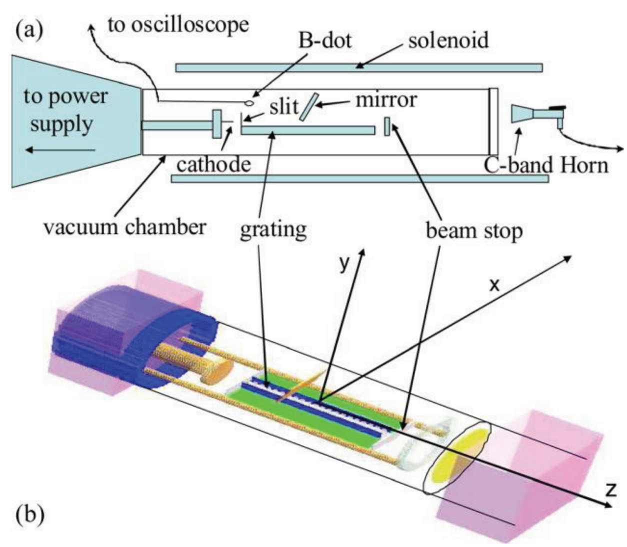

Figure 5: (a) Schematic diagram of the set-up. (b) "MAGIC" simulation geometry. The enclosing solenoid is not shown.

In Figure 5(a) we show a diagram of the experiment, with the essential elements. A movable planar metallic mirror was used to reflect radiation downstream towards a C-band horn placed outside the vacuum chamber. A movable B-dot probe was placed so as to measure B_x in the region upstream from the mirror. Since the vacuum chamber is enclosed in a solenoid, a more complex geometry was used in the simulation volume, which is shown in Figure 5(b).. The pink-colored volumes at both ends indicate "free space", where impinging radiation is absorbed. The solenoid and cathode stalk are represented as conductors and do not absorb radiation.

In Figure 6 we show graphs of the horn power and B_x as functions of time. The presence of the mirror increases the power in the antenna, but has little effect on the fields seen by the probe. Since the antenna had an aperture of $20\ \mathrm{cm}^2$, we estimate a peak power flux of about $110\ \mathrm{W/cm}^2$. Fourier analysis of the probe signal indicates a frequency near 5.2 GHz, as expected.

ISBN 978-3-95450-126-7

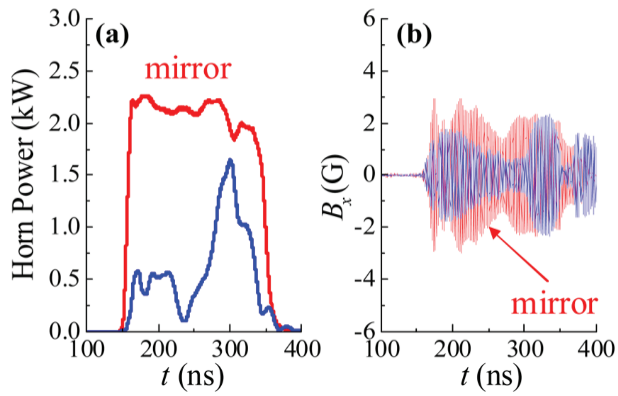

Figure 6: (a) Horn antenna power v. t, with (blue) and without mirror (red). (b) $B_x(t)$ measured by B-dot probe.

In Figures 7(a) and 7(b) we show simulated snapshots of the component B_x in the median z-y plane of the grating. The solenoid, grating, vacuum chamber, and cathode stalk are clearly visible. In 7(a) no mirror is present while in 7(b) one may discern the mirror placed above the seventh period. At the time shown, the field has not reached large values, and is also concentrated at the downstream end. The arrows indicate the paths followed by the SP radiation, and one sees a rough plane-wave structure emerging in 7(b), indicating that the mirror is functioning, even if imperfectly. However, there is considerable reflection occurring at the wall of the solenoid, as well as some radiation creeping under the mirror. In both maps we observe considerable radiation escaping at the upstream end of the grating. There is also some evidence for the second harmonic in 7(a). Unfortunately, our oscilloscope was limited to 6 GHz, so we couldn't investigate this.

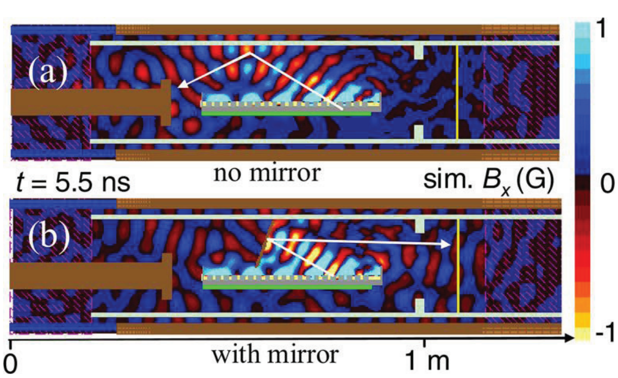

Figure 7: "MAGIC" generated contour maps of the magnetic field component B_x in the median z-y plane. (a) No mirror. (b) With mirror.

CONCLUSION

The results presented here show that in the microwave domain, the use of a grating with sidewalls permits us to obtain coherent SP radiation at the frequency of the surface wave. In this way we attained efficiency of order 10 %, as compared to 0.1 % for operation on the second harmonic. This suggests that the use of gratings with sidewalls will be a necessary feature in the extension of SP FELs to higher frequencies.

REFERENCES

[1] S. J. Smith and E. M. Purcell, Phys. Rev. **92**,1069 (1953).
[2] A. Gover and Z. Livni, Optics Communications **26**, 375 (1978).
[3] J. M. Wachtel, J. Appl. Phys. **50**, 49 (1979).
[4] L. Schächter and A. Ron, Phys. Rev. **A40**, 876 (1989).
[5] C. S. Liu and V. K. Tripathi, IEEE J. Quantum Electron. **35**,1386 (1999).
[6] J.E. Walsh,,J.H. Brownell, J.C. Schwartz,J. Urata, M. F. Kimmitt, Nucl. Instr. And Meth. **A 429** (1999).
[7] H. L. Andrews and C. A. Brau, Phys. Rev. ST Accel. Beams **7**, 070701 (2004).
[8] Vinit Kumar and Kwang-Je Kim, Phys. Rev. **E 73**, 026501 (2006).
[9] B. Goplen, L. Ludeking, D. Smithe, and G. Warren, Computer Physics Communications **87,** 54 (1995).
[10] J. T. Donohue and J. Gardelle, Phys. Rev. ST Accel. Beams **8**, 060702 (2005).
[11] Dazhi Li, Z. Yang, K. Imasaki and Gun-sik Park, Phys. Rev. ST Accel. Beams **9**, 040701 (2006
[12] J. Gardelle, L. Courtois, P. Modin and J. T. Donohue, Phys. Rev. ST Accel. Beams **12**, 110701 (2009).
[13] J. Gardelle, P. Modin and J. T. Donohue, Phys. Rev. Lett. **105**, 224801 (2010).
[14] H.L. Andrews, C. A. Brau, J. D. Jarvis, C. F. Guerin, A. O'Donnell, B. Durant, T. H. Lowell, and M.R. Mross, Phys. Rev. ST Accel. Beams **12**, 080703 (2009).
[15] J. T. Donohue and J. Gardelle, Phys. Rev. ST Accel. Beams **14**, 060709 (2011).
[16] D. Li, K. Imasaki, X. Gao, Z. Yand, and G.S. Park. Appl. Phys. Lett. **91**, 221506 (2007).
[17] Kwang-je Km and V Kumar, Phys. Rev. ST Accel. Beams **10**, 080702 (2007).
[18] B. D. McVey, M. A. Basten, J. H. Booske, J. Joe, and J.E. Scharer, IEEE Trans. Microwave Theory and Techniques, **42**, 995, (1994).
[19] J. T. Donohue and J. Gardelle, Appl. Phys. Lett. **99**, 161112 (2011).
[20] J. Gardelle, P. Modin and J. T. Donohue, Appl. Phys. Lett. **100**, 131103 (2012).

ISBN 978-3-95450-126-7